Journal of Applied Mechanics and Technical Physics, Vol. 44, No. 1, pp. 129–134, 2003

SPEED OF MOTION OF A SHORT-CIRCUIT ARC IN AN INSULATED CONDUCTOR

V. V. Titkov

UDC 538.082/083

The paper deals with different scenarios of electric arc discharge propagation in the ITER tokamak toroidal magnet conductor. Estimates are obtained for the rate of discharge propagation along an insulated conductor and the conditions under which the conductor is cut by a direct current arc with typical values of 10–80 kA*. The modes of a vacuum arc and normal and high-pressure arcs are considered. The analysis was based on steady-state heat- and mass-transfer equations in a combination with the model of evaporation of the Knudsen–Langmuir surface.*

Key words*: electric arc, metal sheath, failure, numerical solution.*

In developing new powerful objects of electric power industry, such as the ITER tokamak [1], which is characterized by rather large (several tens of gigajoules) values of stored electromagnetic energy, investigation of the possible emergency modes is required. The problem of the electromagnetic safety of the ITER includes estimation of the consequences caused by a short-circuit electric arc. Most of the electromagnetic energy is stored in the superconducting windings of the ITER magnet. Therefore, under conditions of a short-circuit arc powered from the magnet, the arc current can reach 70–80 kA in the initial stage and decay in tens of seconds without passage through zero [2]. In fact, these conditions gives rise to a direct current arc, which cannot decay spontaneously. From the viewpoint of possible damage to the environment and the object itself, it is important to estimate the probability of a powerful electric arc damaging the cryostat wall and leaving the superconducting part of the tokamak (Fig. 1).

In the present work, we studied a possible version of development of an accident in which an electric arc arises near the current leads of the toroidal magnet winding and travels along the conductor toward the cryostat wall. The causes of such accidents are not considered here. These can be, for example, electric breakdown due to failure of the solid and vacuum insulation, as a result of which a voltage pulse of about 10–20 kV arises when electromagnetic energy exits the coil. It is necessary to estimate the speed of arc motion along the conductor, which consists of a metal sheath with a plate separating the regions of forward and reverse current (Fig. 1). The current-carrying leads consist of a superconducting cable enclosed in an insulating layer about 1 mm thick. The insulating layer prevents free motion of the arc along the conductor under the action of an electromagnetic force directed from the coil toward the cryostat. This direction of the force is due to the positive sign of the derivative of the inductance of the current circuit formed by the arc and the conductor with respect to the possible direction of arc motion. Therefore, the speed of arc motion along the cable toward the cryostat wall is limited by the rate of failure of the superconducting cable insulation. This mode is maintained as long as the speed of longitudinal motion of the arc is higher than the rate of failure of the cable in the transverse direction (Fig. 2a). Otherwise, the cable will be cut by an electric arc, and arc motion toward the cryostat wall becomes impossible (Fig. 2b). The present paper considers the first of the indicated modes and the conditions of transition to the second mode.

A calculated diagram for the heating of the cable by an electric arc moving along the cable during insulation evaporation is shown in Fig. 3. The main parameters determined in the model considered are the contact spot temperature T_a and the arc propagation speed v. In addition, the following auxiliary parameters are determined: the depth of failure of the metal sheath h_c, the rate of ablation due to insulation evaporation, and the mass rate of formation of metal vapor due to evaporation of the metal sheath of the cable. The value of h_c is the criterion for transition from the surface discharge model to the cut cable model.

St. Petersburg State Technical University, St. Petersburg 195251. Translated from Prikladnaya Mekhanika i Tekhnicheskaya Fizika, Vol. 44, No. 1, pp. 155–162, January–February, 2003. Original article submitted April 26, 2002.

0021-8944/03/4401-0129 $25.00

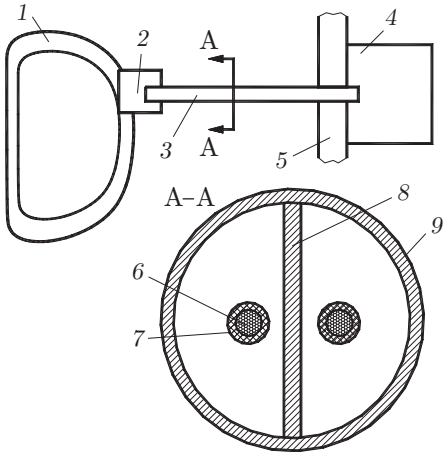

Fig. 1. Supply circuit of the toroidal field coil and a cross section of the supplying conductor: 1) toroidal field coil; 2) terminals; 3) conductor; 4) electric connection housing; 5) cryostat wall; 6) lead of the cable; 7) insulating layer; 8, 9) separating plate and conductor sheath (grounded).

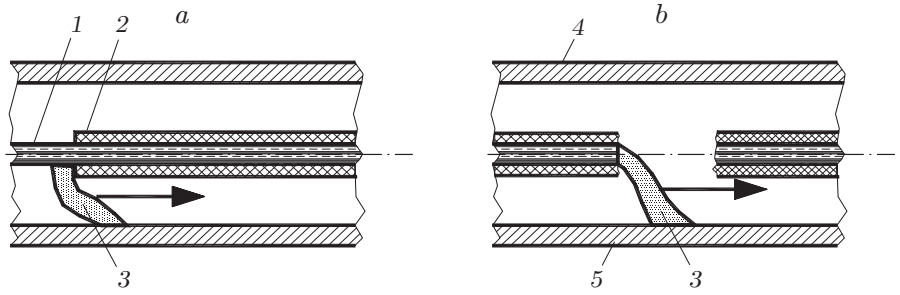

Fig. 2. Modes of interaction of an electric short-circuit arc with the cable surface: surface discharge mode (a) and cut cable mode (b): 1) conducting lead; 2) insulating layer; 3) arc; 4) conductor sheath; 5) separating plate (the arrow denotes the direction of the electromagnetic force).

We assume that the temperature distribution is uniform over the cross section of the cable. Then, the temperature distribution along the cable during arc motion with speed v is given by the formula [3]

$$T(x) = \frac{q}{c\rho_c v A\sqrt{1+4Db/v^2}} \exp\Big(-\frac{v}{2D}(x+|x|\sqrt{1+4Db/v^2}\,)\Big), \tag{1}$$

where $D = \lambda/(\rho_c c)$, λ is the thermal conductivity, ρ_c and c are the density and specific heat of the cable material, v is the arc propagation speed, which is identically equal to the longitudinal rate of pyrolysis of the cable insulation, A is the cross-sectional area of the cable, $b = b_1 + b_2$ is the effective coefficient of heat transfer from the cable surface, where b_1 and b_2 are the convective and radiation components [4]: $b_1 = \alpha p/(c\rho_c A)$ and $b_2 = \sigma_{\rm SB} T_a^3 p_A/(c\rho_c A)$ [$\sigma_{\rm SB} = 5.67051 \cdot 10^{-8}$ W/(m$^4 \cdot$K) is the Stefan–Boltzmann constant, p_A is the perimeter of the cable cross section, T_a is the temperature of the cable at the site of its contact with the arc, α is the heat-transfer coefficient]; q is the heat source power:

$$q = q_{\rm rad} + I\Delta U - \Delta W \tag{2}$$

($q_{\rm rad}$ is the power supplied into the cable by the radiation from the arc plasma). In the case of an atmospheric-pressure electric arc, where local thermodynamic equilibrium occurs in the arc plasma, the power transmitted to the cable by radiation in the gray body approximation is given by [5]

$$q_{\rm rad} = k_F g \sigma_{\rm SB} \pi a_{\rm col}^2 (T^4 - T_a^4), \tag{3}$$

where g is the emissivity of the plasma–electrode system ($0.5 < g < 1$) [5], $a_{\rm col}$ is the radius of the arc column, T and T_a are the plasma temperature in the arc column and the arc spot, respectively, and $k_F \approx 1$ is a coefficient that takes into account the shape of the radiating arc. In the case of a vacuum arc, the role of radiation is inappreciable

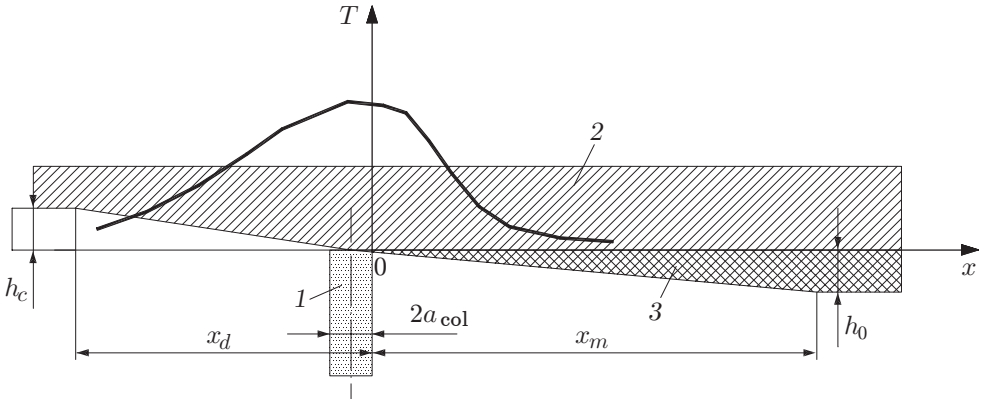

Fig. 3. Calculated diagram of arc motion along the cable surface during insulation failure: 1) arc; 2) conducting lead; 3) insulation.

and energy is released primarily in the electrode region [3]. This is taken into account by the second term $I\Delta U$ in expression (2), where ΔU is the voltage drop near the electrodes, which depends weakly on the arc current. In (2), $\Delta W = \Delta W(T_a, v)$ is the power loss due to evaporation of the insulation ahead of the moving arc spot (region x_m in Fig. 3) and the power loss due to evaporation of the metal sheath of the cable behind the arc spot (region x_d in Fig. 3). (We note that the power loss due to fusion of the cable materials are an order of magnitude smaller than the losses due to evaporation.) In the mode of a surface arc, the depth of failure of the metal sheath of the cable $h_c \ll R_c$ (R_c is the radius of the cable cross section), and the thickness of the insulating layer is $h_0 \ll R_c$. Under these conditions,

$$\Delta W = 2\pi R_c v\Big(\frac{h_c\rho_c\Delta H_c}{N_{\text{A}}M_{c1}} + \frac{h_0\rho_i\Delta H_i}{N_{\text{A}}M_c}\Big). \tag{4}$$

Here the first term describes the power loss due to evaporation of the metal sheath of the cable, the second terms describes the power loss due to insulation evaporation, ρ_c, ΔH_c, and M_{c1} are the density, molar energy of sublimation, and the average atomic weight of the metal sheath material, ρ_i, ΔH_i, and M_c are the same parameters for the insulation material, and N_{A} is the Avogadro number.

To estimate the complete depth of failure to the metal sheath of the cable h_c, we determine the rate of evaporation of the material at a certain point behind the contact spot of the moving arc Fig. 3):

$$\frac{dh}{dt} = \frac{\dot{\Phi}_\rho}{\rho_c}, \tag{5}$$

where $\dot{\Phi}_\rho$ is the flow of the mass evaporating from unit surface. The quantity $\dot{\Phi}_\rho$ is defined by the Knudsen–Langmuir formula [6, 7]

$$\dot{\Phi}_\rho = f_a(P_w(x) - P_0)/\sqrt{2\pi k_{\text{B}}T/M_{c1}}.$$

Here f_a is the attachment factor of about unity (below, for simplicity, we set $f_a = 1$), P_w is vapor saturation pressure, P_0 is the pressure above the surface, and k_{B} is the Boltzmann constant. The vapor saturation pressure is defined by Trawton's law [8] $P_w = C_{\text{T}}\exp(-\Delta H_c/(RT))$, where $C_{\text{T}} = 3.63$ GPa is Trawton's constant and $R = 8.314510$ J/(mole$\cdot$ K) is the universal gas constant. After substitution of the expression for $\dot{\Phi}_\rho$, Eq. (5) can be integrated over time. Because the action parameters at the examined point x vary with time during arc motion, it is convenient to separate the stage of passage of the arc spot above the point x from the subsequent times. Therefore, during the integration of Eq. (5), the integration interval is divided into two parts:

$$h_c = \int\limits_0^{2a/v} \frac{C_{\text{T}}\exp\left[-\Delta H_c/(RT_a)\right] - P}{\rho_c\sqrt{2\pi k_{\text{B}}T_a/M_{c1}}}\,dt + \int\limits_{2a/v}^{\infty} \frac{C_{\text{T}}\exp\left[-\Delta H_c/(RT)\right] - P_0}{\rho_c\sqrt{2\pi k_{\text{B}}T/M_{c1}}}\,dt.$$

Here P is the arc pressure, P_0 is the pressure behind the arc spot, equal to the pressure in the volume of the conductor (in the absence of considerable gas flows from the discharge region, we can set $P_0 = P$).

The first integral on the right side of the expression for h_c can be calculated analytically under the assumption of constant pressure P and temperature T_a within the arc spot. Considering the arc speed along the cable constant v, we convert to the new variable of integration $x = vt$. We obtain

$$h_c = \frac{1}{v\rho_c}\Big(2a_{\text{col}}\,\frac{C_{\text{T}}\exp\left[-\Delta H_c/(RT_a)\right]-P}{\sqrt{2\pi k_{\text{B}}T_a/M_{c1}}} + \int\limits_{-x_d}^{0}\frac{C_{\text{T}}\exp\left[-\Delta H_c/(RT)\right]-P_0}{\sqrt{2\pi k_{\text{B}}T/M_{c1}}}\,dx\Big). \tag{6}$$

In the integral entering into expression (6), the length of the integration interval is determined from the condition that ablation ceases when the saturation pressure becomes equal to ambient pressure, i.e.,

$$C_{\text{T}}\exp\left[-\Delta H_c/(RT_{-x_d})\right] = P_0. \tag{7}$$

We note that the temperature in (6) and (7) is given by expression (1). The temperature of the arc contact spot can be obtained from expression (1), in which the center of the spot corresponds to the coordinate $x = 0$:

$$T_a = (q_{\text{rad}} + I\Delta U - \Delta W)/(c\rho_c vA\sqrt{1+4Db/v^2}\,). \tag{8}$$

Here ΔW is calculated from formula (4).

The speed of arc motion along the cable can be calculated from an expression similar to (6) obtained for insulation failure thickness h_i (the value of h_i is known and is equal to the initial insulation thickness h_0). Then,

$$v = \frac{1}{h_0\rho_i}\int\limits_{0}^{x_m}\frac{C_{\text{T}}\exp\left[-\Delta H_i/(RT)\right]-P_0}{\sqrt{2\pi k_{\text{B}}T/M_c}}\,dx. \tag{9}$$

Here the length of the integration interval is determined by the point of cessation of evaporation, for which the following equation is valid: $C_{\text{T}}\exp\left[-\Delta H_i/(RT_{x_m})\right] = P_0$.

Equations (4), (8), and (9) form a system for the power loss due to evaporation of the materials ΔW, the arc spot temperatures T_a, and the speed of arc spot travel along the cable surface v. The system is solved numerically by bisection with a preliminary analysis of the solution search area. The solution has the form of three nested iterative cycles. with the contact spot temperature determined in the inner cycle and ΔW determined in the outer cycle.

Let us consider examples of calculations carried out for the model described. Because of the large number of physical and design parameters in the present problem, it is not possible to obtain a solution in generalized form or to use similarity methods to represent the result in compact form. Therefore, the proposed model was used to analyze the particular example of the ITER toroidal magnet conductor. In test calculations, the following initial data were used: effective cross-sectional area of the cable $A = 0.002$ m^2 corresponding to a cable diameter of 3 cm, specific heat $c = 50$ J/(kg$\cdot$ K) and thermal conductivity $\lambda = 50$ W/(m$\cdot$ K) typical of steel, densities of the cable and insulation materials $\rho_c = 8000$ kg/m^3 and $\rho_i = 1500$ kg/m^3, emissivity of the surface $g = 1$, average atomic weight $M_c = M_{c1} = 4.7\cdot 10^{-26}$ kg, convective heat-transfer coefficient $\alpha = 0$–200 W/(m$^2\cdot$ K), perimeter of the cable cross section $p = 0.15$ m, insulation thickness $h_0 = 1$ mm, molar energies of sublimation of the cable materials $\Delta H_c = 450$ kJ/mole and $\Delta H_i = 300$ kJ/mole, cathode (anode) voltage drop $\Delta U = 8$–20 V, arc current $I = 10$–80 kA, radius and temperature of the arc column $a_{\text{col}} = 0.01$–0.02 m and $T = 1000$–$20{,}000$ K, and gas concentration in the arc column 10^{20}–10^{28} m^{-3}. The calculations were carried out for the following values of the pressure P_0 in a large volume (behind the arc column): 0.1 Pa (vacuum arc), 0.1 MPa (atmospheric pressure arc), and 1 MPa (high-pressure arc).

Vacuum Arc. A vacuum arc is characterized by a significant difference in the thermal power released on the anode and the cathode [3]. If the cable surface is the cathode, the power supplied into the cable is determined by the arc current and the cathode voltage drop (in the case of steel electrodes, $\Delta U \leqslant 20$ V). The results of numerical solution of system (4), (8), (9) for $q_{\text{rad}} = 0$ and $I = 10$–80 kA are given in Fig. 4. Figure 4 shows the results of calculation for the case where the cable surface is the anode. In this case, according to [3], the power released in the contact area is approximately five times higher than that in the cathode region of the arc. As follows from Fig. 4, the values of v and T_a for the case of anode and cathode contacts between the arc and the cable differ slightly. In this case, $v_{\max} \lesssim 1$ cm/sec and $T_{\max} \approx 5000$ K. The depth of failure depends strongly on the power released at the arc contact spot. In the case of cathode contact and $I = 50$–60 kA, the depth of failure is sufficient for cable cutting, and for anode contact, the corresponding value of the current is 10 kA.

Atmospheric-Pressure Arc. When a short-circuit closure arc is drawn at atmospheric or high pressure, the anode and cathode voltage drop is $\Delta U \approx 10$ V, and the plasma radiation plays a more significant role than in a

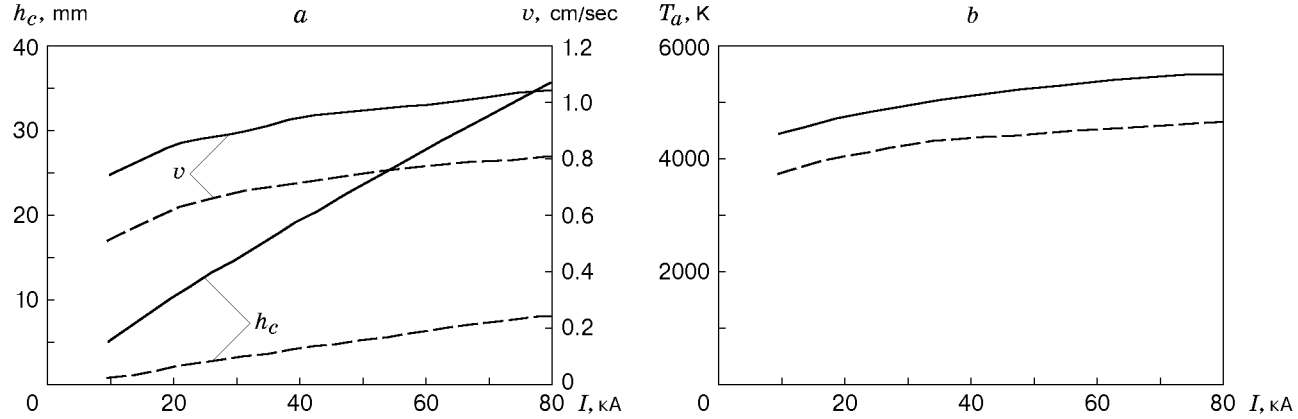

Fig. 4. Speed of motion along the cable, depth of failure of the metal sheath (a), and contact spot temperature (b) versus vacuum arc current for the cases of anode (solid curves) and cathode (dashed curves) contact.

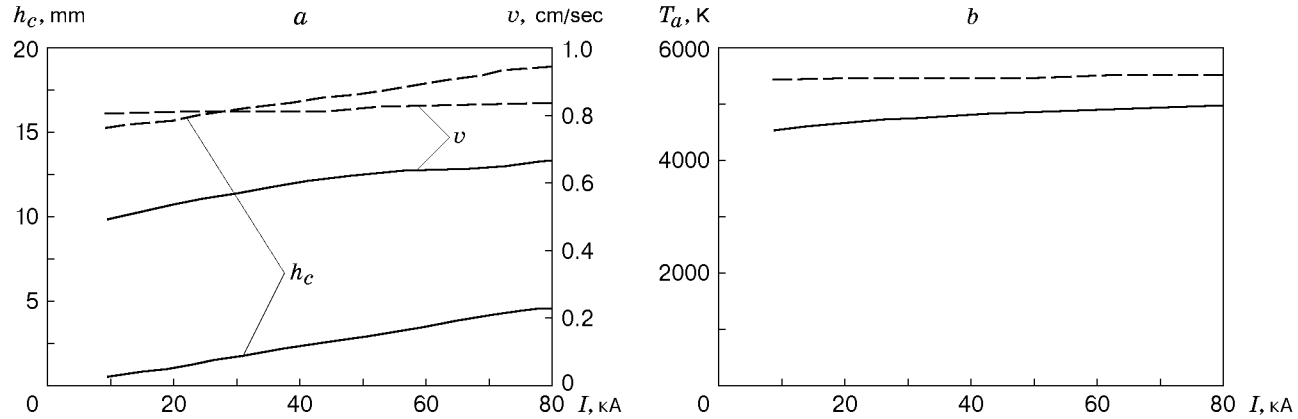

Fig. 5. Speed of motion along the cable, depth of failure of the metal sheath (a) and contact spot temperature (b) versus atmospheric-pressure arc current for $T = 10{,}000$ (solid curves) and 20,000 K (dashed curves).

vacuum arc. In this case, Eq. (7) should include the component describing power transfer by radiation in the contact region (3). Usually, the temperature of an atmospheric-pressure open-flame arc plasma is close to 10,000 K [9]. However, heat removal from the arc inside the conductor into the ambient medium is hindered compared with an open-flame arc. Therefore, calculations for the model considered were performed for an atmospheric-pressure arc with two arc plasma temperatures: 10,000 and 20,000 K (Fig. 5). In this case, the second value, can be considered as the upper bound for the temperature of an arc burning in a large volume.

As in the case of a vacuum arc, the speed of contact spot travel along the cable surface does not exceed 1 cm/sec, and the depth of failure is slightly smaller than that in the case of anode contact of a vacuum arc. Nevertheless, for the upper bound of the plasma temperature (20,000 K), the depth of failure is sufficiently large for the arc to cut the cable. At $T = 10{,}000$ K, the calculated depth of failure is much smaller and does not exceed 5 mm for current values of 10–80 kA. However, the speeds of arc motion in both cases are close (maximum difference 0.8 cm/sec). Comparison of the calculation results at $T = 10{,}000$ and 20,000 K suggests that the probability of cable cutting is higher for the case where the heat removal from the arc to the ambient space is hindered. This situation arises in the bounded volume of the conductor.

High-Pressure Arc. A high-pressure arc was studied for the case where the pressure in the volume of the cable was equal to 10 atm. Calculation results are given in Fig. 6. A high-pressure arc is characterized by a strong dependence of the depth of sheath failure on plasma temperature. As in the cases considered previously, the calculated speed of arc motion along the cable does not exceed 1 cm/sec. For the most probable average temperature of a high-pressure arc plasma of 20,000 K, the depth of failure is so great that the cable will be cut and the arc will be closed between the cable cut off and the separating plate of the conductor (see Fig. 2b). As in the previous modes, the temperature in the contact area between the arc and the cable surface is in the range of 5000–6000 K.

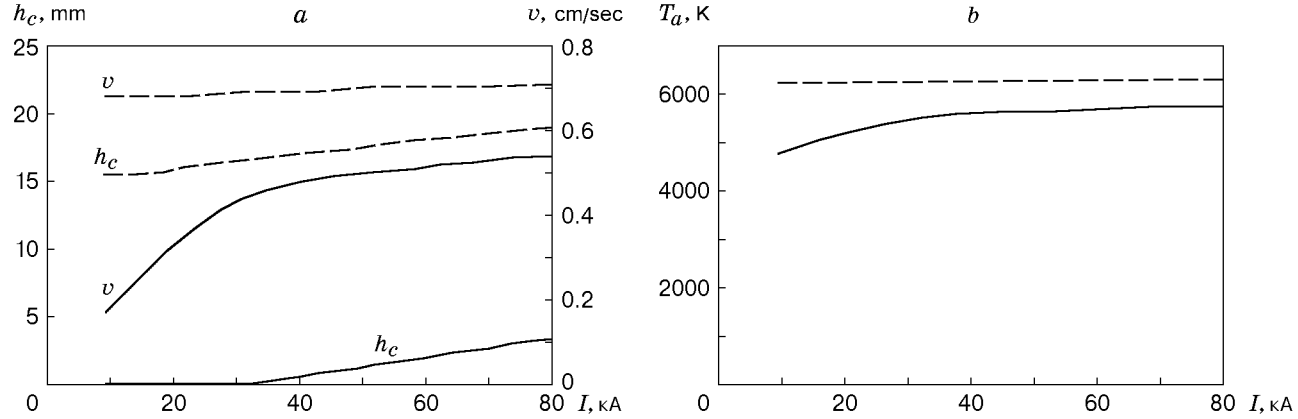

Fig. 6. Speed of motion along the cable, depth of failure of the metal sheath (a), and contact spot temperature (b) versus high-pressure arc current for $T = 10{,}000$ (solid curves) and 20,000 K (dashed curves).

Calculations using the model considered show that the parameters of the process depend substantially on the radius of the arc column. In particular, an increase in the diameter of the arc column to 3 cm (in the previous calculations 2 cm) significantly changes the conditions of interaction between the arc and the cable: the arc speed decreases to 0.48 cm/sec, and the depth of failure exceeds the cable diameter equal to 30 mm.

The effect of variation of the insulation thickness on the rate of surface discharge propagation along the cable is insignificant: an increase in the insulation thickness to 4 mm (for conditions of the previous calculation) leads to a 6% decrease in the rate of discharge propagation along the cable.

Thus, for a conductor with an isolated lead, the surface arc discharge mode with $I = 10$–80 kA is most probable for a vacuum arc provided that the cable surface is the cathode. In this case, the speed of arc motion along the cable is determined by the ablation of the insulation and does not exceed 1 cm/sec. For anode contact of a vacuum arc and the cable, the cross sectional dimensions of the failure are commensurable with the cable radius, which means cutting of the cable by the arc. The surface discharge mode with the same speed of motion takes place for an atmospheric-pressure arc with a characteristic temperature of 10,000 K. In the case of a high-pressure arc with hindered heat exchange, where the arc plasma temperature exceeds 20,000 K, the surface discharge mode is impossible, as in the case of anode contact with a vacuum arc. Thus, in all electric arc modes in the cable, the rate of surface discharge propagation along the cable is insignificant. Therefore, an accident of this type will apparently lead to metal short-circuiting (taking into account the possible strains accompanying fusion of the cable material) or to the cutting of the cable by the electric arc and fixing of one of its terminal on the cable cut-off.

REFERENCES

1. F. Iida, K. Yoshida, S. Stoner, and A. Tesini "ITER magnet interface system," in: *Proc. of the 15th Int. Conf. on Magnet Technol.*, Part 1, S.n., Beiging, China (1997), pp. 433–436.
2. D. P. Ivanov, B. N. Kolbasov, D. K. Kurbatov, et al., "Qualitative analysis of accidents possible in ITER magnets," *Plasma Devices Operations*, **7**, 205–217 (1999).
3. V. V. Frolov (ed.), *Theory of Welding Processes* [in Russian], Vysshaya Shkola (1988).
4. V. A. Karkhin, *Thermal Fundamentals of Welding* [in Russian], Leningrad State Tech. Univ., Leningrad (1990).
5. R. V. Mitin, "Stationary and pulsed high- and hyperhigh-pressure arcs and methods of their diagnostics," in: *Properties of a Low-Temperature Plasma and Methods of Its Diagnostics* [in Russian], Nauka, Novosibirsk (1977), pp. 105–138.
6. B. V. Alekseev and A. M. Grishin, *Physical Gas Dynamics of Reactive Media* [in Russian], Vysshaya Shkola (1985).
7. N. V. Afanas'ev and O. F. Shlenskii, *Short-Duration Thermal Stability of Nonmetallic Materials* [in Russian], St. Petersburg State Tech. Univ., St. Petersburg (1995).
8. É. É. Shpil'rain and P. M. Kissel'man, *Fundamentals of the Theory of Thermal Properties of Materials*, [in Russian], Énergia, Moscow (1977).
9. G. A. Kukekov, *High-Voltage Alternating-Current Switches* [in Russian], Énergiya, Leningrad (1972).